

Effect of biomass features on oxygen transfer in Conventional Activated Sludge and Membrane BioReactor systems

Marco Capodici^a, Santo Fabio Corsino^a, Daniele Di Trapani^{a,*}, Michele Torregrossa^a, Gaspare Viviani^a

^a Department of Engineering, University of Palermo, Viale delle Scienze Ed. 8, 90128 Palermo, ITALY

*Corresponding author: Daniele Di Trapani E-mail address: daniele.ditrapani@unipa.it Phone: +39 09123896552

Abstract

The aim of the present study was to compare the oxygen transfer efficiency in a conventional activated sludge and a membrane bioreactor system. The oxygen transfer was evaluated by means of the oxygen transfer coefficient $(k_{La})_{20}$ and α -factor calculation, under different total suspended solids concentration, extracellular polymeric substances, sludge viscosity and size of the flocs. The $(k_{La})_{20}$ and α -factor showed an exponential decreasing trend with total suspended solid, with a stronger $(k_{La})_{20}$ dependence in the conventional activated sludge than the membrane bioreactor. It was noted that the $(k_{La})_{20}$ in the conventional activated sludge become comparable to that in membrane bioreactor when the TSS concentration in the conventional activated sludge was higher than 5 gTSS L⁻¹. Operating under high carbon to nitrogen ratio, the $(k_{La})_{20}$ increased in both conventional activated sludge and membrane bioreactor because of the sludge deflocculation and a weaker dependence of $(k_{La})_{20}$ with total suspended solid was noted.

The results indicated that the most important parameters on the oxygen transfer efficiency were in order: the total suspended solid concentration, flocs size, sludge viscosity, the protein to polysaccharides ratio and extracellular polymeric substances content.

Based on the influence of the main biomass features affecting the $(k_{La})_{20}$ and considering the typical operating conditions in both systems, those of membrane bioreactor appeared to be more favorable to oxygen transfer efficiency compared to conventional activated sludge process.

Keywords: Aeration efficiency, activated sludge properties, EPS, Membrane Bioreactor, Oxygen transfer; Energy consumption

34

35 **1. Introduction**

36 Energy saving has become one of the most debated topic in the field of any industrial activity,
37 including also wastewater treatment plants (WWTP) (Henriques and Catarino, 2017; Torregrossa et
38 al., 2018). Aeration is the most energy-intensive operation in wastewater treatment, amounting to 45-
39 75% of plant energy costs (Rosso et al., 2008; Li et al., 2017; Wu et al., 2019); this operation is crucial
40 in WWTPs, since dissolved oxygen (DO) represents an essential factor in biological processes for the
41 treatment of both municipal and industrial wastewater (Tang et al., 2015).

42 Over recent years, several aeration machineries manufactories have developed innovative devices
43 with the aim to increase the aeration efficiency in terms of mass of oxygen transferred per unit energy
44 required (Zheng et al., 2018). In parallel, the plant facilities were upgraded by equipping those
45 machineries that are more efficient in order to maximize the amount of oxygen that transfers from air
46 to water (Hewawasam et al., 2017). Nevertheless, oxygen transfer process does not depend entirely
47 on diffusers or aerators design, but also on the biomass characteristics (Germain and Stephenson,
48 2005). Indeed, several investigations have linked the limitation to the oxygen transfer to solids
49 concentrations and viscosity of mixed liquor, as well as the content of soluble microbial products
50 (SMP) and extracellular polymeric substances (EPS) (Germain et al., 2007). Therefore, a better
51 understanding of the energy saving strategies requires deeper investigations on the oxygen transfer
52 phenomena in relation with biomass characteristics.

53 Whilst on the one hand the energy-saving necessity led operators and manufactories to implement
54 strategies and devices with low environmental impact, on the other, the more stringent environmental
55 laws has driven researchers toward advanced technologies that are more energy-consuming
56 (Krzeminski et al., 2012). Among these, the membrane bioreactors (MBRs) technology is largely
57 considered the first alternative to the conventional activated sludge (CAS) process because of the
58 higher effluent quality, compatible with the water reuse requirements, and the lower footprint
59 (Hoinkis et al., 2012). Nonetheless, in MBR the main power requirement comes from aeration, which

60 is used for oxygen supply and membrane scouring to prevent fouling formation (Germain et al.,
61 2007). Therefore, the improvement of aeration design with a reduction of the energy consumption is
62 of great importance to push the widespread application of MBRs (Xu et al., 2017).

63 In MBR systems, the biomass features may differ significantly from that of CAS plants, including
64 the higher viscosity and EPS content, the smaller particle size, etc. (Di Bella et al., 2010). Similarly,
65 some operating parameters, like the hydraulic retention time (HRT), the solid retention time (SRT),
66 the food to microorganisms ratio (F/M), might be significantly different to that of CAS (Bertanza et
67 al., 2017). All these factors highly affect the oxygen transfer efficiency, which is usually expressed
68 in terms of global oxygen transfer coefficient (k_{LA}); moreover, the alpha-factor (α -factor), defined as
69 the ratio of k_{LA} under process and clean water conditions, accounts for the effects of activated sludge
70 features (Verrecht, 2010). Some of the above parameters are known to be associated with lower
71 oxygen transfer efficiency, as TSS concentration, viscosity and EPS content, whereas others, like
72 particle size, HRT and F/M, are favorable to oxygen transfer (Germain et al., 2007). The main
73 differences between CAS and MBR in terms of biomass features and operating conditions, as well as
74 the different contribution to oxygen transfer efficiency, make difficult the possibility to assess a
75 comprehensive analysis on aeration efficiency by default. In several studies, it was speculated that
76 the main factor affecting the difference between oxygen transfer in CAS and MBR systems is the
77 flocs size (Fan et al., 2017). For this reason, because the mass transfer is linked to the contact area
78 between gas and liquid phase, the MBR should be favored because of the smaller particles size
79 (Germain et al., 2007). Nevertheless, a comparison between the impact of the particles size on the
80 oxygen transfer efficiency in CAS and MBR was not investigated so far and, in general, very limited
81 data of k_{LA} and α -factor for MBRs have been reported (Xu et al., 2017).

82 In this light, the aim of this study was to analyze the oxygen transfer in CAS and MBR systems. In
83 detail, the study was aimed at assessing:

84 1) the comparison between the k_{LA} in CAS and the MBR at different TSS concentration;

- 85 2) the impact of the activated sludge flocs size on the oxygen transfer efficiency in CAS and
86 MBR;
87 3) the influence of the main biomass features on the k_{La} .

88

89 **2. Material and methods**

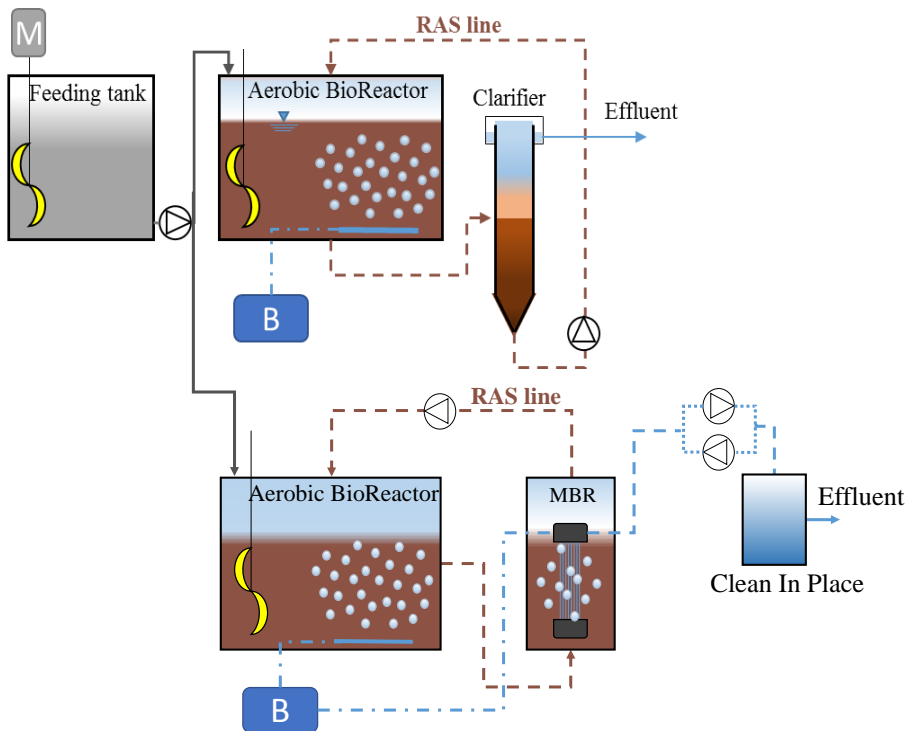
90 *2.1 CAS and MBR plant configuration*

91 As aforementioned, in the present study two bench scale plants, one CAS and one MBR, were started-
92 up to study the oxygen transfer efficiency. The CAS plant consisted in one aerobic reactor (25 L of
93 volume) and a clarifier (3 L of volume, $7.84 \cdot 10^{-3} \text{ m}^2$ of surface). The MBR was realized according to
94 the submerged side-stream configuration, consisting in one aerobic reactor (24.5 L of volume) and
95 another one (2.5 L of volume) where an ultra-filtration (UF) hollow fibers (HF) membrane module
96 (Zee-Weed[®], specific area = 0.1 m^2 and nominal porosity = $0.04 \text{ }\mu\text{m}$, courtesy of GE,) was placed.
97 The aerobic reactors of both the CAS and MBR were geometrically identical ($L \times l \times h = 0.35 \text{ m} \times$
98 $0.35 \text{ m} \times 0.20 \text{ m}$) and were equipped with two equal fine bubble air diffusers each, for dissolved
99 oxygen supply. The airflow rate was maintained constant at 6 L min^{-1} . Fibers scouring was achieved
100 by supplying air to the membrane, in order to mitigate the fouling formation.

101 Both the systems were fed with a synthetic medium with a flow rate of 1 L h^{-1} , resulting in a HRT of
102 approximately 25 h. The synthetic wastewater was stored into a continuously mixed tank from which
103 it was fed through two peristaltic pumps to the aerobic reactors of the CAS and MBR systems. In the
104 CAS, the activated sludge from the bottom of the clarifier was recycled to the aerobic reactor with a
105 flow rate of 2 L h^{-1} , whereas in the MBR the retentate from the membrane compartment was recycled
106 to the aerobic reactor with a flow rate of 6 L h^{-1} . The permeate flux was kept almost to $18 \text{ L m}^{-2} \text{ h}^{-1}$,
107 while the net effluent flow rate was equal to 1 L h^{-1} . The membrane filtration cycle was divided into
108 5 min of filtration and 1 min of backwashing, by pumping back a small volume of permeate through
109 the membrane.

110 A schematic layout of the CAS and MBR systems is depicted in Figure 1.

111



112

113 2.2 Experimental campaign

114 The experimental campaign had a duration of 70 days and it was divided into two different periods,
115 named Period 1 and Period 2. During Period 1 (50 days), the CAS and MBR were fed with a synthetic
116 wastewater having a C/N/P ratio of approximately 100:10:2. During Period 2 (20 days), the amount
117 of nitrogen and phosphorous in the synthetic medium was decreased, resulting in a C/N/P ratio of
118 100:2.5:0.5, in order to favour the activated sludge deflocculation in the CAS because of unbalanced
119 nutrients condition. The main features of the synthetic wastewater are reported in Table 1.

120

Parameter	Unit	Period 1	Period 2
COD (as sodium acetate)	mg L ⁻¹	382.8±20.1	392.4±26.3
NH ₄ -N (as ammonium chloride)	mg L ⁻¹	37.8±3.9	18.9±3.2
PO ₄ -P (as hydrogen potassium phosphate)	mg L ⁻¹	7.9±1.2	3.8±0.7
C:N:P	-	100:10:2	100:2.5:0.5

121

122 Both plants were seeded with conventional activated sludge collected from the aeration tank of the
123 “Acqua dei Corsari” wastewater treatment plant located in Palermo (Italy), with initial concentrations
124 of 3 gTSS L⁻¹ and 6 gTSS L⁻¹ for CAS and MBR, respectively.

125

126 2.3 Determination of the oxygen transfer coefficient

127 The oxygen transfer coefficient (k_{LA}) was evaluated within the same aerobic reactors, first with tap
128 water (before the inoculum) in order to calculate the (k_{LA}) referred to clean water conditions, then
129 with the biomass at different TSS concentrations. All the tests were performed in batch conditions
130 and at room temperature according to the non-steady-state batch test (Stenstrom et al., 2006). Before
131 starting the oxygen transfer measurement, the dissolved oxygen in water was removed. More
132 precisely, in the test with tap water a chemical oxygen demand (sodium sulphite and cobalt chloride
133 as catalyst) was added to the water, whereas in the test with biomass deoxygenation was achieved
134 because of the oxygen consumption by bacteria. The air blower was then switched on and, after a
135 while, the dissolved oxygen concentration reached the saturation value due to the aeration
136 (reoxygenation phase) at an airflow rate of 6 L min⁻¹. The dissolved oxygen concentration was
137 measured through an oxygen probe (WTW CelOX-325) coupled to an oximeter (WTW
138 MULTI340i).

139 The standard model for evaluating oxygen transfer is given by Equation 1.

$$140 \quad \frac{dC}{dt} = k_{LA} \cdot (C_S - C_0) \quad (eq. 1)$$

141 where:

- 142 • C = dissolved oxygen concentration (mg/L);
- 143 • t = time (min);
- 144 • k_{LA} = volumetric mass transfer coefficient (min⁻¹);
- 145 • C_S = dissolved oxygen saturation concentration at steady state (mg L⁻¹);
- 146 • C_0 = dissolved oxygen concentration at time zero (mg L⁻¹).

147 The equation used for data analysis with nonlinear regression is given in Equation 2 and is a derivation
148 from Equation 1:

$$149 \quad C = C_S - (C_S - C_0) \cdot e^{(-k_L a \cdot t)} \quad (eq. 2)$$

150 By plotting the C values achieved during the reoxygenation phase in a graph $\ln(C_S - C)/(C_S - C_0)$ vs t ,
151 the volumetric mass transfer coefficient was obtained as the slope of the regression line.

152 The k_{La} was then referred at the temperature of 20 °C by using the equation 3:

$$153 \quad (k_L a)_{20} = (k_L a)_T \cdot 1.024^{T-20} \quad (eq. 3)$$

154 The α -factor was obtained as the ratio of process to clean water conditions, as follows (eq. 4):

$$155 \quad \alpha = \frac{(k_L a)_{process,water}}{(k_L a)_{clean,water}} \quad (eq. 4)$$

156 The oxygen transfer coefficient was periodically measured within the aerobic reactors of both CAS
157 and MBR plants at different TSS concentrations, by concentrating or diluting the biomass samples.

158

159 *2.4 Analytical methods*

160 Extracellular polymeric substances extraction was carried out in accordance with the Heating Method
161 (Le-Clech et al., 2006). Therefore, for both the extracted SMP and EPS fractions, the carbohydrate
162 and protein concentrations were determined according to the phenol–sulphuric acid method with
163 glucose as the standard (DuBois et al., 1956) and by the Folin method with bovine serum albumin as
164 the standard (Lowry et al., 1951), respectively.

165 The particle size distribution of both the activated sludge from CAS and MBR was measured by
166 means of a high-speed image analyses sensor (Sympatec Qicpic) that provided the particle size
167 distribution and the granulometric curve. The average size of the activated sludge flocs was calculated
168 as the diameter of the particles corresponding to the 50% of the granulometric distribution. The
169 morphology of the activated sludge flocs was evaluated with microscopic image observations
170 performed by a phase contrast microscope (BX-53-Olympus).

171 Microscopic observations were performed under phase contrast at 100× and 1000× magnifications.
172 The filamentous microorganisms were morphologically identified using the Eikelboom classification
173 system. Filamentous microorganism abundance and dominance were estimated according to the
174 literature (Jenkins et al., 2004).

175 The activated sludge viscosity was evaluated by means of a rotational rheometer (Brookfield digital
176 viscometer, model DV-E) equipped with concentric cylinders and an adapter for low viscosity at
177 constant temperature (20°C).

178

179 *2.5 Statistical analysis*

180 In order to evaluate the influence of the main biomass features (TSS concentration, EPS content and
181 composition, sludge viscosity and size of the flocs) on the oxygen transfer coefficient, the multiple
182 regression analysis was performed. More precisely, the dependent variable was the oxygen transfer
183 coefficient, whereas the independent variables were the biomass features. The regression coefficients
184 (*Beta coefficients*) was used to evaluate the degree of influence of each biomass feature on the $(k_{La})_{20}$,
185 according to the literature (Germain et al., 2007).

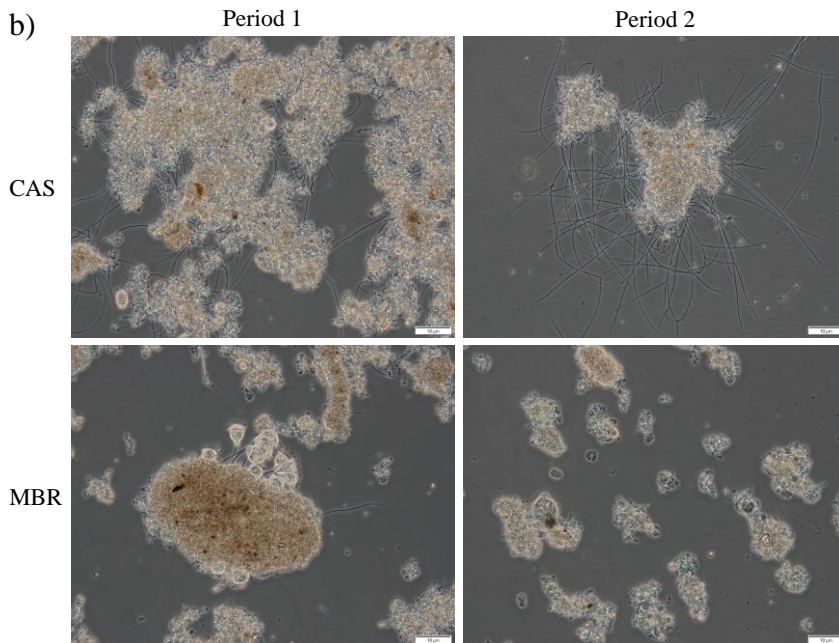
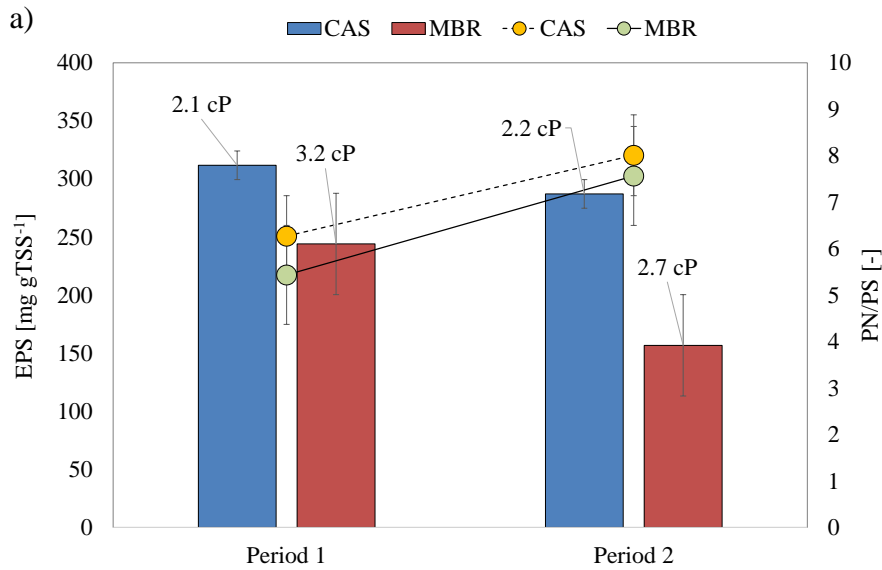
186

187 **3. Results and discussion**

188 *3.1 Features of the activated sludge in the CAS and MBR*

189 The main features of the activated sludge in the CAS and MBR in Period 1 and Period 2, in terms of
190 EPS content and composition, flocs size and morphology, are shown in Figure 2.

191



192

193

194 The average EPS content of CAS was of approximately 311 mg g⁻¹TSS in Period 1, whereas it slightly
 195 decreased to 287 mg g⁻¹TSS in Period 2. Similarly, the EPS content of MBR decreased from 244 mg
 196 g⁻¹TSS to 156 mg g⁻¹TSS from Period 1 to Period 2, indicating that the nutrient unbalance determined
 197 a decrease in the EPS secretion by bacteria in both systems. The EPS composition changed as well
 198 from Period 1 to Period 2. More precisely, the protein (PN) to carbohydrate (PS) ratio (PN/PS)
 199 increased from 6.2 to 8 and from 5.4 to 7.5 in the CAS and MBR, respectively. Therefore, the nutrient
 200 unbalance caused a simultaneous decrease in the amount of the total EPS and the enrichment in the
 201 proteinaceous fraction of the extracellular polymeric matrix.

202 The activated sludge viscosity did not change significantly from Period 1 to Period 2 in the CAS (2.1
203 cP vs 2.2 cP), whereas it slightly decreased in the MBR (3.2 cP vs 2.7 cP).

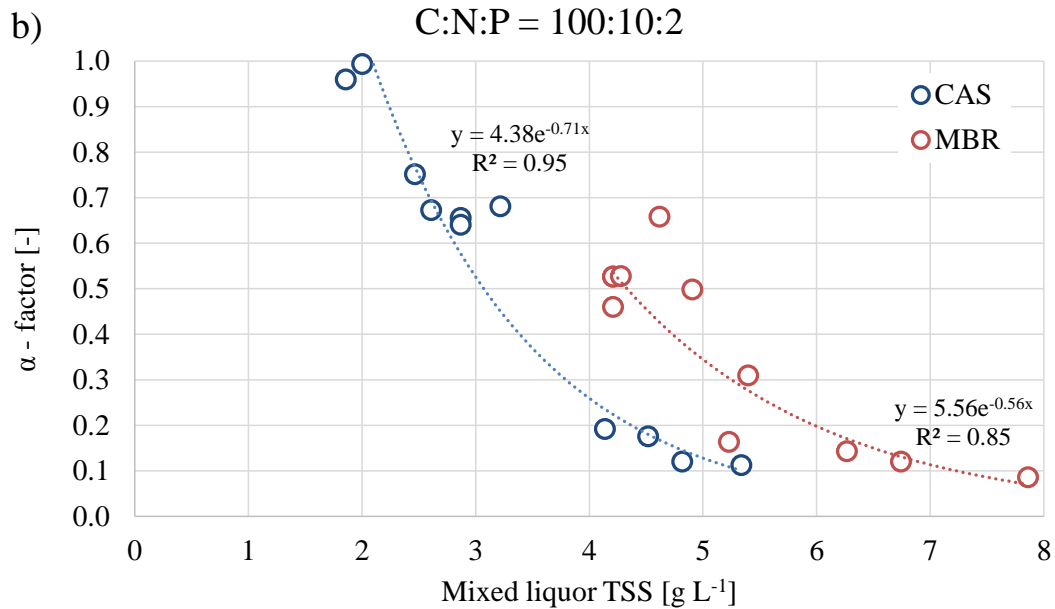
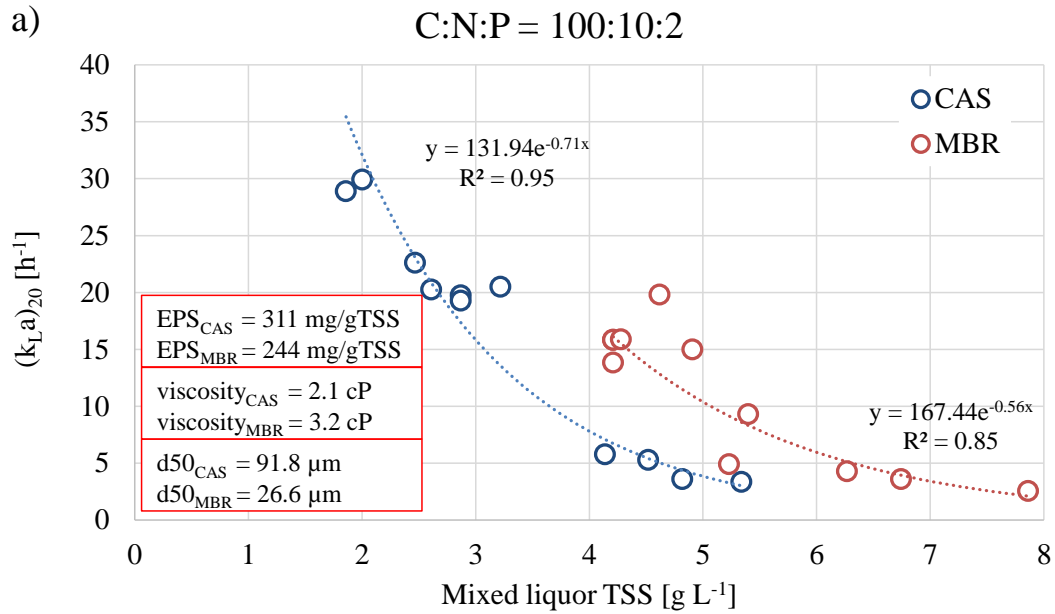
204 The morphology of the activated sludge flocs significantly changed from Period 1 to Period 2. Indeed,
205 in Period 1 the flocs were slightly irregular but compact in the CAS (average size of 91.8 μm), with
206 a common presence of filamentous bacteria (*Nocardia* sp, *Microthrix Parvicella* and *Type 0675*). In
207 Period 2, the activated sludge morphology changed to open-flocs structure (average size of 25.1 μm)
208 with a predominance of filamentous bacteria like *Type 021N*, *Type 0965* and *Thiotrix* sp. In the MBR,
209 the activated sludge flocs were very small but with a regular and compact shape. The size of the flocs
210 was close to 27 μm on average in Period 1 because of the deflocculation effect exerted by the
211 membrane. In Period 2, average size of the activated sludge flocs further decreased to approximately
212 12 μm , whereas no significant changes in the morphology was observed. Filamentous bacteria like
213 *Type 021N*, *Type 0965* and *Thiotrix* sp, were found dominant even in the MBR, although their effect
214 on the flocs morphology was marginal compared to that in the CAS.

215

216 3.2 Oxygen transfer coefficient in the CAS and MBR: Period 1

217 Biomass with TSS concentrations ranging from 1.5 gTSS L⁻¹ and 5.3 gTSS L⁻¹ and from 4.2 gTSS L⁻¹
218 ¹ and 7.8 gTSS L⁻¹ were examined in the CAS and MBR, respectively, during Period 1. The oxygen
219 transfer coefficient and the α -factor obtained in the CAS and MBR at different TSS concentration in
220 Period 1 are depicted in Figure 3.

221



222

223 The $(k_{La})_{20}$ coefficient showed an exponential decrease with the increase in TSS in both the CAS
 224 and MBR (Fig. 3a), in good agreement with previous findings (Wu et al., 2019). In general, the $(k_{La})_{20}$
 225 values obtained by Wu and co-workers were slightly lower compared to what achieved in the present
 226 study for a similar TSS concentration range. These variations could be likely due to different testing
 227 conditions (e.g. aeration intensity, diffuser typology, reactor geometrical features, mixed intensity,
 228 etc.). The $(k_{La})_{20}$ decreased sharply from 30 h^{-1} to less than 5 h^{-1} when the TSS concentration
 229 increased from 2 gTSS L^{-1} to 4 gTSS L^{-1} in the CAS, whereas further increases in TSS did not
 230 produced significant decrease in $(k_{La})_{20}$. Similarly, the $(k_{La})_{20}$ coefficient in the MBR decreased from

231 approximately 16 h^{-1} to 4 h^{-1} when the TSS concentration increased from 4 gTSS L^{-1} to 8 gTSS L^{-1} .
232 The α -factor (Fig. 3b) was of approximately 0.96 in the CAS at 2 gTSS L^{-1} , whereas it significantly
233 decreased in the range between 3 gTSS L^{-1} and 4 gTSS L^{-1} standing at a steady value of approximately
234 0.15. In the MBR the maximum values of the α -factor were observed at 4 gTSS L^{-1} ($\alpha=0.5$), whereas
235 it decreased to less than 0.1 at TSS concentrations higher than 7 gTSS L^{-1} .
236 By comparing the exponential decreasing trends observed in the CAS and MBR, it was noted that the
237 dependence of $(k_{LA})_{20}$ on TSS was stronger in the CAS than the MBR. Under the typical operating
238 TSS concentration in CAS (3 gTSS L^{-1}) and MBR (8 gTSS L^{-1}), the obtained results confirmed that
239 oxygen transfer coefficient was lower in the MBR (3.6 h^{-1} vs 20 h^{-1}). Nevertheless, it is worth noting
240 that the $(k_{LA})_{20}$ values in the CAS become comparable with that in MBR when the TSS concentration
241 in the CAS was higher than 5 gTSS L^{-1} , which is typical of plants operating under extended aeration.
242 Within a range of TSS between 4 gTSS L^{-1} and 6 gTSS L^{-1} the $(k_{LA})_{20}$ value resulted significantly
243 higher in the MBR, thereby suggesting that under similar operating conditions the features of the
244 activated sludge features in the MBR were more favorable to oxygen transfer.
245 Differences between the activated sludge features in the CAS and MBR were observed in terms of
246 EPS content and average size of the flocs. Indeed, although the mixed liquor viscosity was higher in
247 the MBR on average, the specific EPS content was higher in the CAS ($311 \text{ mg g}^{-1}\text{TSS}$ vs $244 \text{ mg g}^{-1}\text{TSS}$),
248 as well as the average size of the activated sludge flocs, which resulted approximately equal
249 to $92 \mu\text{m}$ and $27 \mu\text{m}$ in the CAS and MBR, respectively. The above results suggested that the oxygen
250 transfer coefficient and the α -factor, in addition to TSS concentration, strictly depend on the EPS
251 content and size of the activated sludge flocs. These results are in good agreement with the literature,
252 in which the negative effect of the EPS on $(k_{LA})_{20}$ was previously observed by several researchers
253 (Mueller et al., 2002; Germain et al., 2007).
254 It is reasonable to speculate that the decrease of $(k_{LA})_{20}$ in the MBR, due to the increase of TSS
255 concentration, was compensated by the lower EPS content and the smaller size of the activated sludge

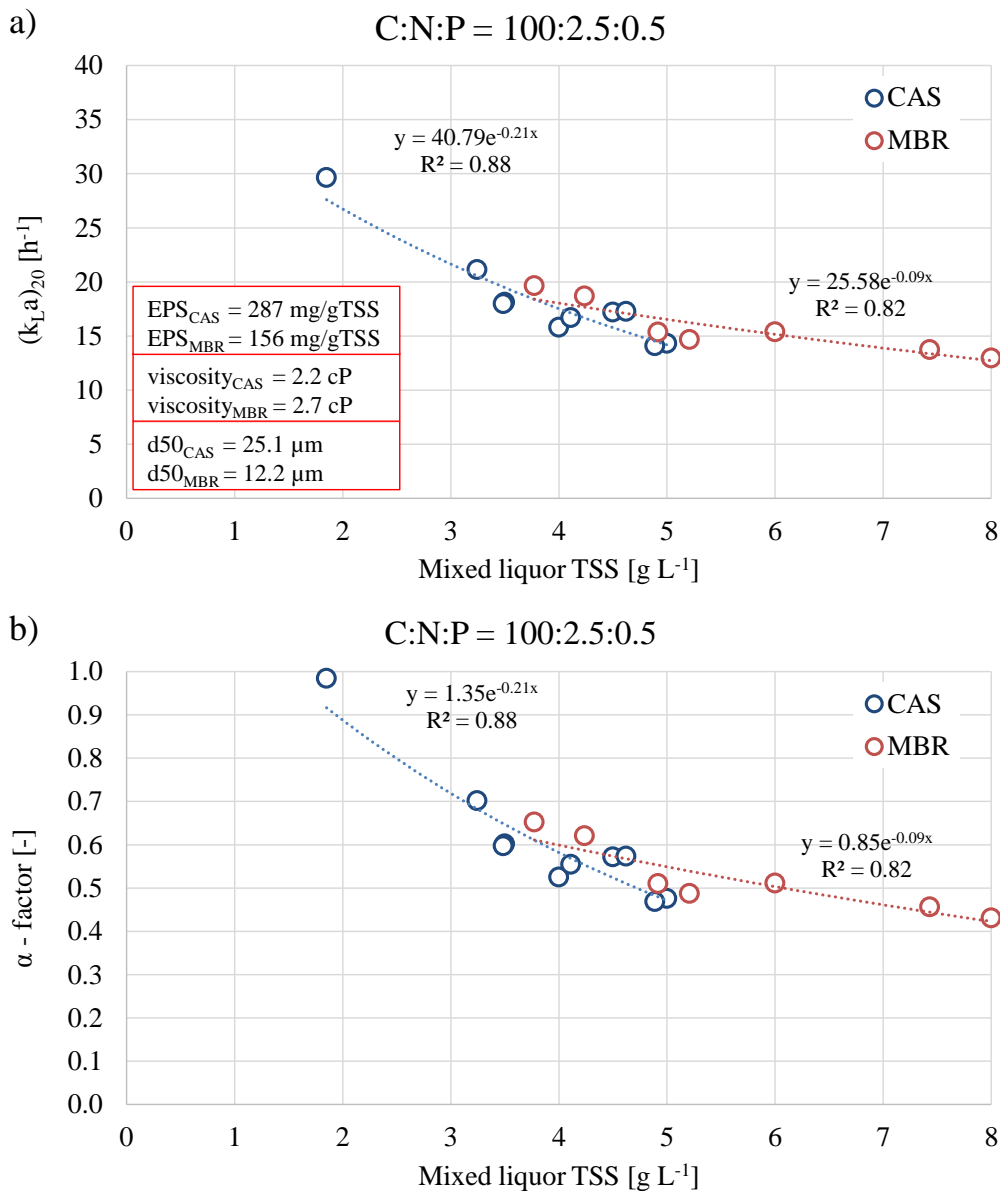
256 flocs. Therefore, the latter might be the reason of the weaker relationship of the $(k_{La})_{20}$ with TSS in
 257 the MBR compared to the CAS system (Freitas and Teixeira, 2001).

258

259 *3.3 Effect of activated sludge deflocculation on oxygen transfer: Period 2*

260 In Period 2 the amount of nitrogen and phosphorous in the synthetic influent wastewater was
 261 decreased in order to simulate the effects of a nutrients unbalanced wastewater on the oxygen transfer
 262 efficiency. Figure 4 depicts the relationship between the $(k_{La})_{20}$ (Fig. 4a) and the α -factor (Fig. 4b)
 263 with the TSS concentration in the CAS and MBR in Period 2.

264



265

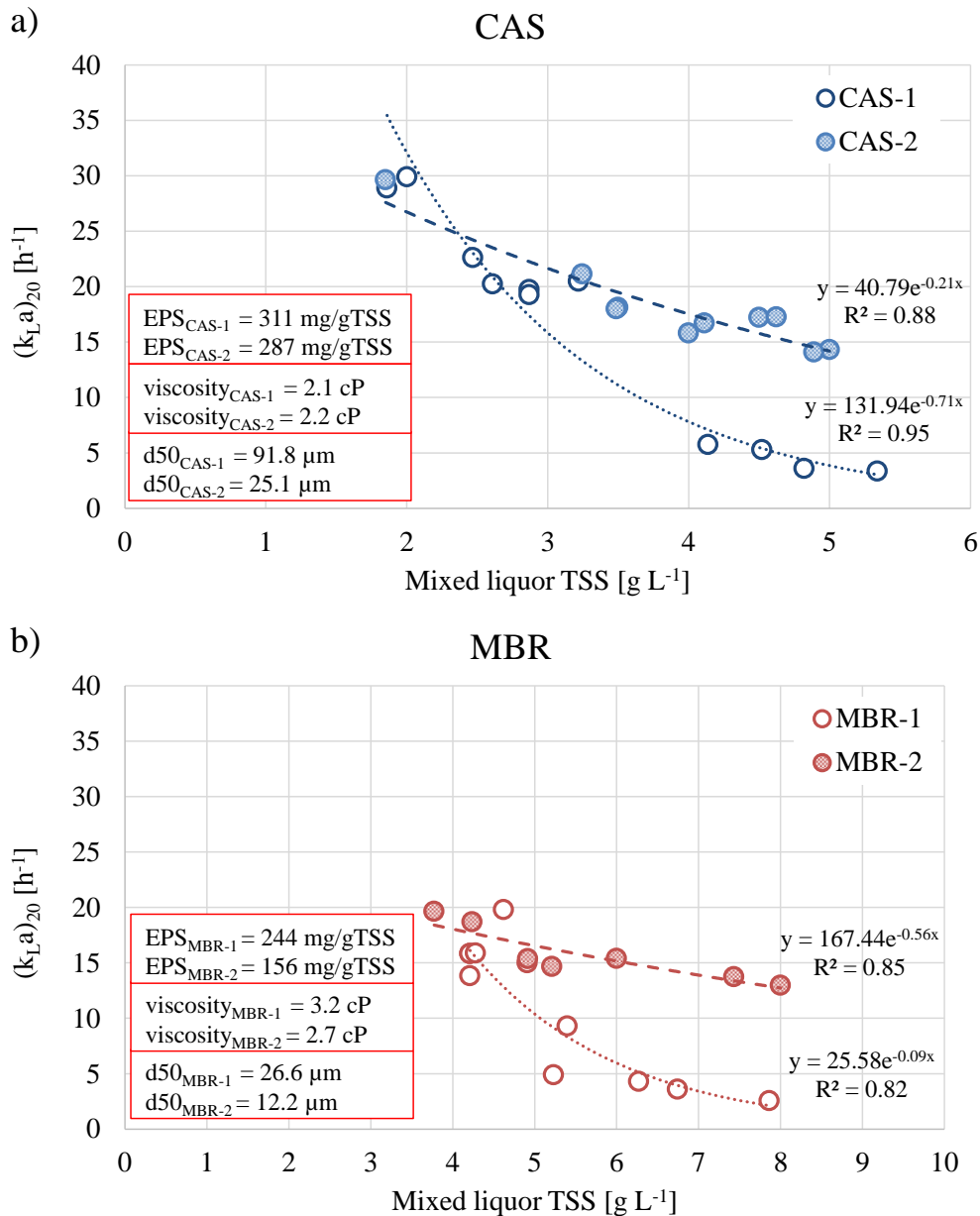
266 The results shown in Figure 4 indicated that $(k_{LA})_{20}$ increased in both CAS and MBR plants because
267 of the nutrients unbalance. Overall, a weaker dependence of $(k_{LA})_{20}$ with TSS was observed compared
268 to Period 1. Indeed, although the $(k_{LA})_{20}$ showed the same exponential decreasing trend observed in
269 Period 1, the $(k_{LA})_{20}$ values obtained in Period 2, at equal TSS concentration, significantly increased.
270 The $(k_{LA})_{20}$ in the CAS decreased from 30 h^{-1} to less than 15 h^{-1} when the TSS concentration increased
271 from 2 gTSS L^{-1} to 4 gTSS L^{-1} , whereas in Period 1 it decreased to less than 5 h^{-1} within the same
272 range of TSS. At higher TSS the $(k_{LA})_{20}$ did not decreased further, standing at a constant value of
273 approximately 15 h^{-1} . Similarly, the $(k_{LA})_{20}$ decreased from 20 h^{-1} to approximately 13 h^{-1} in the MBR
274 when the TSS concentration increased from 4 g TSS L^{-1} to 8 g TSS L^{-1} , showing a weaker dependence
275 with TSS compared to CAS system. The α -factor decreased from 0.97 to 0.48 when the TSS
276 concentration increased from 2 g TSS L^{-1} to 5 g TSS L^{-1} , whereas in the MBR it decreased from 0.65
277 to 0.42 within a range of TSS between 3.6 g TSS L^{-1} and 8 g TSS L^{-1} .

278 Overall, the differences between the oxygen transfer in the CAS and MBR significantly reduced in
279 Period 2. Because of the nutrients unbalance, the physical properties of the activated sludge
280 significantly changed in both the systems. The average EPS content decreased from $311\text{ mg g}^{-1}\text{TSS}$
281 to $287\text{ mg g}^{-1}\text{TSS}$ and from $244\text{ mg g}^{-1}\text{TSS}$ to $156\text{ mg g}^{-1}\text{TSS}$ in the CAS and the MBR, respectively.
282 Similarly, the size of the activated sludge flocs significantly decreased in the CAS from $91.8\text{ }\mu\text{m}$ to
283 $25.1\text{ }\mu\text{m}$, indicating the occurrence of a massive deflocculation, whereas in the MBR the size of the
284 flocs decreased to a lesser extent from $26.6\text{ }\mu\text{m}$ to $12.2\text{ }\mu\text{m}$. The achieved result indicated that the
285 decrease in the EPS content and the size of activated sludge flocs significantly improved the oxygen
286 transfer in both the systems. Moreover, both the $(k_{LA})_{20}$ and the α -factor resulted very similar in both
287 systems. Previous studies highlighted significantly poorer oxygen transfer efficiency in presence of
288 filamentous organisms, concerning in particular to the *Thiothrix eikelboomi*, due to the enhancement
289 of sludge viscosity and particular cell surface (Liu et al., 2018; Wu et al., 2019). In the present study,
290 despite in Period 2 it was observed a significant growth of filamentous organisms (including the

291 *Thiothrix eikelboomi*), their negative effect on oxygen transfer could be masked by the beneficial
 292 variation of other parameters, such as EPS, open floc structure and average floc size.

293 A comparison of the oxygen transfer, in terms of $(k_{La})_{20}$, with the TSS in Period 1 and Period 2 in the
 294 CAS and MBR is depicted in Figure 5.

295



296

297 In the CAS, at TSS lower than 2.5 g TSS L⁻¹ the $(k_{La})_{20}$ was slightly higher in Period 1, whereas at
 298 higher TSS concentration the $(k_{La})_{20}$ was higher in Period 2. As aforementioned, the dependence of
 299 the $(k_{La})_{20}$ with TSS significantly reduced in Period 2 and their relationship became almost linear.

300 The above observations were replicable for the MBR, although the increase in the $(k_{LA})_{20}$ was lower
301 compared to the CAS.

302 The higher increasing trend of $(k_{LA})_{20}$ observed in the CAS system was likely due to the greater
303 deflocculation effect observed in this system. In view of a slight decrease in the specific EPS content
304 (<10%), the only characteristic of the activated sludge flocs that significantly changed in the CAS
305 from Period 1 to Period 2 was the average size of the bioaggragates and the higher abundance of
306 filamentous bacteria. Therefore, it can be stated that the increase in the $(k_{LA})_{20}$ in the CAS was mainly
307 driven by the activated sludge deflocculation. In previous literature, it was observed a negative impact
308 of the filamentous overgrowth on the oxygen transfer (Liu et al., 2018). The authors noted a
309 significant worsening in the oxygen transfer efficiency due to the filamentous microorganisms that
310 caused the increase of the EPS content in the activated sludge and its viscosity. Nevertheless, the
311 authors only speculated that the filamentous overgrowth caused an increase in the activated sludge
312 viscosity, thus decreasing the oxygen transfer efficiency. In the present study, the filamentous
313 overgrowth observed mainly in the CAS during Period 2, did not cause a significant increase in the
314 activated sludge viscosity. In contrast, it modified the sludge morphology creating open-flocs
315 structure having much greater specific surface area and greater exposure to the bulk solution.

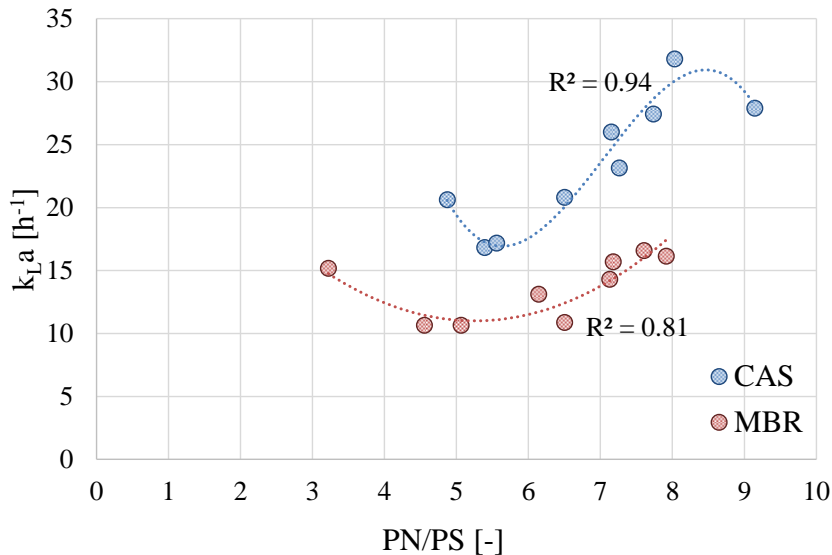
316 The effect of the decrease in the floc size was lower in the MBR, because it was smaller since the
317 beginning. Nevertheless, it was compensated by the decrease of the EPS content, close to 36%. This
318 result was in good agreement with previous literature, which reported the negative impact of the bio-
319 surfactants like EPS in the oxygen transfer efficiency (Capodici et al., 2014).

320 Based on the above results, it can be concluded that the nutrient unbalance improved the oxygen
321 transfer in both the CAS and MBR, although the mechanisms involved in the increase in the $(k_{LA})_{20}$
322 were different.

323

324 *3.4 Impact of EPS composition on oxygen transfer*

325 The above results indicated that the decrease of the EPS content improved the oxygen transfer. In
326 light of this, with the aim to better clarify the role of the EPS compounds on the oxygen transfer
327 behavior, the $(k_{LA})_{20}$ was correlated with the protein (PN) to carbohydrates (PS) ratio (PN/PS) (Fig.
328 6).



329 The $(k_{LA})_{20}$ and the PN/PS showed a good correlation in both the CAS and MBR plants. More
330 precisely, the $(k_{LA})_{20}$ significantly increased when the PN/PS was higher than 5, showing an
331 exponential trend in both systems. The $(k_{LA})_{20}$ almost doubled in the CAS when the PN/PS increased
332 from 5 to 8, whereas it increased for approximately 50% in the MBR. Therefore, the increase of
333 protein in the EPS matrix was found to be favorable to oxygen transfer. This result was in contrast
334 with previous literature (Germain et al., 2007), where the EPS component that influenced positively
335 the oxygen transfer was found to be the carbohydrate. Germain and co-workers observed that the
336 carbohydrates of the EPS increased flocs porosity and therefore the oxygen diffusivity. In the present
337 study, the highest PN/PS was observed in Period 2 in both systems, when, because of the filamentous
338 overgrowth and the deflocculation, the floc porosity likely increased independently of EPS
339 composition. As previously discussed, the abundance of filamentous bacteria in Period 2 caused the
340 change in the activated sludge morphology to open-flocs structure that was likely favorable to oxygen
341 transfer. Besides, it is worth mentioning that the prevalence of the proteins over the carbohydrates in
342 the EPS matrix increased the sludge hydrophobicity, because of the hydrophobic nature of the
343

344 proteinaceous molecules (Ras et al., 2013). Given the hydrophobic nature of the air bubbles (Shi et
345 al., 2014), it is possible to speculate that the increase in the proteinaceous fraction of the EPS matrix,
346 improved the oxygen transfer because of the establishment of hydrophobic interaction between the
347 activated sludge flocs enriched in proteins and the air bubbles (Ferreira et al., 2010; Mena et al.,
348 2011). Therefore, the in $(k_{LA})_{20}$ in addition to TSS, EPS content and floc size, was found to be
349 dependent of the protein content of the extracellular polymeric matrix.

350

351 *3.5 Relative influence of the biomass features on $(k_{LA})_{20}$*

352 Based on the above considerations, the main features of activated sludge that affected the $(k_{LA})_{20}$ were
353 the TSS, the total EPS content, the PN/PS, the sludge viscosity and the average size of the flocs. In
354 order to evaluate their degree of influence on the oxygen transfer coefficient, a multiple regression
355 analysis was carried out considering the values of $(k_{LA})_{20}$ obtained during the entire experiment. The
356 beta coefficients and the statistical significance parameters obtained by the regression analysis are
357 reported in Table 2.

358

Parameter	CAS	MBR
TSS	-4.48	-3.01
EPS	-0.86	-0.50
PN/PS	0.68	0.98
Viscosity	-1.03	-1.75
Flocs size	-1.62	-2.37
F	31.6	14.5
p-level	<0.05	<0.05

359

360 The obtained results indicated that the degree of influence of the investigated parameters for both the
361 systems were in order: the TSS concentration, flocs size, viscosity, PN/PS and EPS content. More
362 precisely, the TSS, the EPS, the viscosity and the flocs size had a negative influence, meaning that an
363 increase in these parameter led to a decrease of the $(k_{LA})_{20}$, whereas the only parameter having a
364 positive influence was the PN/PS. As afore discussed, the TSS concentration had a higher influence

365 on $(k_{LA})_{20}$ in the CAS than the MBR, as well as the EPS. In contrast, the activated sludge viscosity,
366 the flocs size and the PN/PS had a greater influence in the MBR.

367 Based on the typical operating conditions of CAS and MBR systems, the activated sludge viscosity
368 is generally higher in the MBR, because of the higher TSS concentration they operate (Germain et
369 al., 2007), as well as the average size of the flocs is significantly lower in the MBR (Campo et al.,
370 2017). Moreover, because of the higher sludge retention time and the lower F/M, the amount of EPS
371 is lower, whereas that of proteins in relation to carbohydrates in the EPS matrix is higher in the MBR.
372 Indeed, endogenous metabolic condition imposed by the low F/M, are reported to produce a selective
373 enrichment of proteins in the EPS, due to the biodegradation of the carbohydrates that from a
374 molecular point of view are structurally more simple than proteins (Duan et al., 2014). In contrast, in
375 CAS systems, although the TSS concentration is lower, the amount of EPS is higher than MBR
376 because of the higher F/M.

377 Based on the afore discussed degrees of influence of the main biomass features affecting the $(k_{LA})_{20}$,
378 the operating conditions in MBR systems and its activated sludge features, appeared to be more
379 favorable to oxygen transfer efficiency compared to CAS systems. Nevertheless, an excessive
380 deviation of the above reported parameters from the ranges investigated in the present study could
381 led to different results because of the increase of the degree of influence of such parameter on the
382 oxygen transfer efficiency.

383

384 **Conclusions**

385 A comparison between the oxygen transfer efficiency in CAS and MBR was performed in the present
386 study. The $(k_{LA})_{20}$ and α -factor showed exponential decreasing trends with TSS in the CAS and MBR,
387 even if it was noted that the dependence of both parameters on TSS was stronger in the CAS than the
388 MBR. Although under the typical operating conditions in terms of TSS concentration in the CAS and
389 MBR the oxygen transfer coefficient was lower in the MBR (3.6 h^{-1} vs 20 h^{-1}), it was noted that the
390 $(k_{LA})_{20}$ values were higher in the MBR within a range of TSS between 4 gTSS L^{-1} and 6 gTSS L^{-1} .

391 The achieved results indicated that under similar operating conditions the features of the activated
392 sludge flocs in the MBR were more favorable to oxygen diffusion process because of the smaller
393 particle size.

394 Moreover, the results indicated that the TSS, the EPS, the viscosity and the flocs size had a negative
395 influence on the $(k_{LA})_{20}$, whereas the only parameter having a positive influence was the PN/PS. The
396 TSS concentration had a greater influence on $(k_{LA})_{20}$ in the CAS than the MBR, as well as the EPS.
397 In contrast, the activated sludge viscosity, the flocs size and the PN/PS had a greater influence in the
398 MBR.

399 Based on the degrees of influence of the main biomass features affecting the $(k_{LA})_{20}$ and considering
400 the typical operating conditions in both systems, those of the MBR appeared to be more favorable to
401 oxygen transfer efficiency compared to CAS.

402

403 **References**

404 Bertanza, G., Canato, M., Laera, G., Vaccari, M., Svanström, M., Heimersson, S., 2017. A
405 comparison between two full-scale MBR and CAS municipal wastewater treatment plants:
406 techno-economic-environmental assessment. *Environ. Sci. Pollut. Res.* 24, 17383–17393.
407 doi:10.1007/s11356-017-9409-3

408 Campo, R., Capodici, M., Di Bella, G., Torregrossa, M., 2017. The role of EPS in the foaming and
409 fouling for a MBR operated in intermittent aeration conditions. *Biochem. Eng. J.* 118, 41–52.
410 doi:10.1016/j.bej.2016.11.012

411 Capodici, M., Di Bella, G., Nicosia, S., Torregrossa, M., 2014. Effect of chemical and biological
412 surfactants on activated sludge of MBR system: Microscopic analysis and foam test. *Bioresour.*
413 *Technol.* 177, 80–86. doi:10.1016/j.biortech.2014.11.064

414 Di Bella, G., Durante, F., Torregrossa, M., Viviani, G., 2010. Start-up with or without inoculum?
415 Analysis of an SMBR pilot plant. *Desalination* 260, 79–90. doi:10.1016/j.desal.2010.04.063

- 416 Duan, L., Song, Y., Yu, H., Xia, S., Hermanowicz, S.W., 2014. The effect of solids retention times
417 on the characterization of extracellular polymeric substances and soluble microbial products in
418 a submerged membrane bioreactor. *Bioresour. Technol.* 163, 395–398.
419 doi:10.1016/j.biortech.2014.04.112
- 420 DuBois, M., Gilles, K. a., Hamilton, J.K., Rebers, P. a., Smith, F., 1956. Colorimetric method for
421 determination of sugars and related substances. *Anal. Chem.* 28, 350–356.
422 doi:10.1021/ac60111a017
- 423 Fan, H., Liu, X., Wang, H., Han, Y., Qi, L., Wang, H., 2017. Oxygen transfer dynamics and activated
424 sludge floc structure under different sludge retention times at low dissolved oxygen
425 concentrations. *Chemosphere.* doi:10.1016/j.chemosphere.2016.10.137
- 426 Ferreira, A., Ferreira, C., Teixeira, J.A., Rocha, F., 2010. Temperature and solid properties effects on
427 gas-liquid mass transfer. *Chem. Eng. J.* 162, 743–752. doi:10.1016/j.cej.2010.05.064
- 428 Freitas, C., Teixeira, J.A., 2001. Oxygen mass transfer in a high solids loading three-phase internal-
429 loop airlift reactor. *Chem. Eng. J.* 84, 57–61. doi:10.1016/S1385-8947(00)00274-6
- 430 Germain, E., Nelles, F., Drews, A., Pearce, P., Kraume, M., Reid, E., Judd, S.J., Stephenson, T., 2007.
431 Biomass effects on oxygen transfer in membrane bioreactors. *Water Res.* 41, 1038–1044.
432 doi:10.1016/j.watres.2006.10.020
- 433 Germain, E., Stephenson, T., 2005. Biomass characteristics, aeration and oxygen transfer in
434 membrane bioreactors: Their interrelations explained by a review of aerobic biological
435 processes. *Rev. Environ. Sci. Biotechnol.* doi:10.1007/s11157-005-2097-3
- 436 Henriques, J., Catarino, J., 2017. Sustainable value - an energy efficiency indicator in wastewater
437 treatment plants. *J. Clean. Prod.* 142, 323-330. doi.org/10.1016/j.jclepro.2016.03.173.

- 438 Hewawasam, C., Matsuura, N., Maharjan, N., Hatamoto, M., Yamaguchi, T., 2017. Oxygen transfer
439 dynamics and nitrification in a novel rotational sponge reactor. *Biochem. Eng. J.* 128, 162–167.
440 doi:10.1016/j.bej.2017.09.021
- 441 Hoinkis, J., Deowan, S.A., Panten, V., Figoli, A., Huang, R.R., Drioli, E., 2012. Membrane bioreactor
442 (MBR) technology - A promising approach for industrial water reuse, in: *Procedia Engineering*.
443 pp. 234–241. doi:10.1016/j.proeng.2012.01.1199
- 444 Jenkins, D., Richard, M.G., Daigger, G.T., 2004. *MANUAL on the CAUSES and CONTROL of*
445 *ACTIVATED SLUDGE BULKING, FOAMING, and OTHER SOLIDS SEPARATION*
446 *PROBLEMS.*
- 447 Krzeminski, P., Van Der Graaf, J.H.J.M., Van Lier, J.B., 2012. Specific energy consumption of
448 membrane bioreactor (MBR) for sewage treatment. *Water Sci. Technol.* 65, 380–392.
449 doi:10.2166/wst.2012.861
- 450 Le-Clech, P., Chen, V., Fane, T.A.G., 2006. Fouling in membrane bioreactors used in wastewater
451 treatment. *J. Memb. Sci.* doi:10.1016/j.memsci.2006.08.019
- 452 Li, W., Li, L., Qiu, G., 2017. Energy consumption and economic cost of typical wastewater treatment
453 systems in Shenzhen, China. *J. Clean. Prod.* 163, S374-S378.
454 doi.org/10.1016/j.jclepro.2015.12.109
- 455 Liu, G., Wang, J., Campbell, K., 2018. Formation of filamentous microorganisms impedes oxygen
456 transfer and decreases aeration efficiency for wastewater treatment. *J. Clean. Prod.* 189, 502–
457 509. doi:10.1016/j.jclepro.2018.04.125
- 458 Lowry, O.H., Rosebrough, N.J., Farr, A.L., Randall, R.J., 1951. Protein measurement with the Folin-
459 Phenol Reagent. *J. Biol. Chemistry* 193, 265–275.

- 460 Mena, P., Ferreira, A., Teixeira, J.A., Rocha, F., 2011. Effect of some solid properties on gas-liquid
461 mass transfer in a bubble column. *Chem. Eng. Process. Process Intensif.* 50, 181–188.
462 doi:10.1016/j.cep.2010.12.013
- 463 Mueller, J.A., Boyle, W.C., Popel, H.J., 2002. *Aeration: Principles and Practice*. CRC Press. Boca
464 Raton, USA.
- 465 Ras, M., Lefebvre, D., Derlon, N., Hamelin, J., Bernet, N., Paul, E., Girbal-Neuhauser, E., 2013.
466 Distribution and hydrophobic properties of Extracellular Polymeric Substances in biofilms in
467 relation towards cohesion. *J. Biotechnol.* 165, 85–92. doi:10.1016/j.jbiotec.2013.03.001
- 468 Rosso, D., Larson, L.E., Stenstrom, M.K., 2008. Aeration of large-scale municipal wastewater
469 treatment plants: State of the art. *Water Sci. Technol.* doi:10.2166/wst.2008.218
- 470 Shi, C., Chan, D.Y.C., Liu, Q., Zeng, H., 2014. Probing the hydrophobic interaction between air
471 bubbles and partially hydrophobic surfaces using atomic force microscopy. *J. Phys. Chem. C*
472 118, 25000–25008. doi:10.1021/jp507164c
- 473 Stenstrom, M.K., Leu, S.-Y. (Ben), Jiang, P., 2006. *Theory to Practice: Oxygen Transfer and the New*
474 *ASCE Standard. Proc. Water Environ. Fed.* 2006, 4838–4852.
475 doi:10.2175/193864706783762931
- 476 Thang, B., Qiu, B., Huang, S., Yang, K., Bin, L., Fu, F., Yang, H. 2015. Distribution and mass transfer
477 of dissolved oxygen in a multi-habitat membrane bioreactor. *Bioresour. Technol.* 182, 323-328.
478 doi.org/10.1016/j.biortech.2015.02.028
- 479 Torregrossa, D., Hernández-Sancho, F., Hansen, J., Cornelissen, A., Popov, T., Schutz, G., 2018.
480 Energy saving in wastewater treatment plants: A plant-generic cooperative decision support
481 system. *J. Clean. Prod.* 167, 601–609. doi:10.1016/j.jclepro.2017.08.181

- 482 Verrecht, B., Maere, T., Nopens, I., Brepols, C., Judd, S. 2010. The cost of a large-scale hollow fibre
483 MBR, *Water Res.* 44, 5274–5283. doi:10.1016/j.watres.2010.06.054.
- 484 Wu., X., Huang, J., Lu, Z., Chen, G., Wang, J., Liu, G. 2019. *Thiothrix eikelboomii* interferes oxygen
485 transfer in activated sludge. *Water Res.* 151, 134-143. doi.org/10.1016/j.watres.2018.12.01
- 486 Xu, Y., Zhu, N., Sun, J., Liang, P., Xiao, K., Huang, X. 2017. Evaluating oxygen mass transfer
487 parameters for large-scale engineering application of membrane bioreactors. *Proc. Biochem.* 60,
488 13-18. doi.org/10.1016/j.procbio.2017.05.020
- 489 Zheng, Z., Sun, D., Li, J., Zhan, X., Gao, M., 2018. Improving oxygen transfer efficiency by
490 developing a novel energy-saving impeller. *Chem. Eng. Res. Des.* 130, 199–207.
491 doi:10.1016/j.cherd.2017.12.021
- 492
- 493

494 **FIGURE CAPTIONS**

495 **Figure 1:** Layout of the CAS and MBR

496 **Figure 2:** Average EPS content, composition, and activated sludge viscosity (a), microscopic
497 observation of the sludge in the CAS and MBR during Period 1 and Period 2.

498 **Figure 3:** Oxygen transfer coefficient (a) and α -factor vs TSS in CAS and MBR in Period 1

499 **Figure 4:** Oxygen transfer coefficient (a) and α -factor vs TSS in CAS and MBR in Period 2

500 **Figure 5:** Comparison between the $(k_{La})_{20}$ in Period 1 and Period 2 in the CAS (a) and MBR (b).

501 **Figure 6:** Relationship between the $(k_{La})_{20}$ and the PN/PS ratio of the EPS in the CAS and MBR

502

503

504

505

506 **TABLE LEGENDS**

507 **Table 1:** Features of the synthetic wastewater

508 **Table 2:** Beta coefficients and statistical significance parameters obtained by regression analysis for

509 $(k_{La})_{20}$

510

511